Water Practice & Technology Vol 15 No 2
doi: 10.2166/wpt.2020.016

Experimental study and flow analysis on a new design of water-retaining sluice gate

Wenrong Tu[a], Shibiao Fang[b,c,*] and Zhilin Sun[d]

[a] College Of Civil Engineering and Architecture, Zhejiang University, Hangzhou 310058, People's Republic of China

[b] Shenzhen Research Institute, China University of Geosciences, Shenzhen 518057, China

[c] College of Marine Science and Technology, China University of Geosciences, 388 Lumo Road, Wuhan 430074, China

[d] Ocean college, Zhejiang University, Hangzhou, 310058, China

*Corresponding author. E-mail: wuyibiaobiao@163.com

Abstract

As a water-retaining structure, the hydro-automatic flap gate (HFG) has advantages, such as easy operation, simple structure, attractive appearance, cheaper investment, and simple installation and maintenance compared to traditional gates. As such, the flow pattern analysis and flow rate analysis on this hydraulic structure have important engineering significance. In this paper, an experimental study was carried out for testing the water flow during the opening process of a bottom shaft driving flap gate. Three different opening velocities (once in 20 years, once in 50 years, once in 100 years) were selected for obtaining detailed characteristics. Then the space-time change laws of velocity and other hydraulic parameters of gate, gate pier and stilling pool were described. Moreover, the results of the flow regimes under conditions of once in 20 years, once in 50 years, once in 100 years were compared with each other. The findings and conclusions of this paper provide the basis for the project implementation in a sediment-laden river, and provide reference for other similar projects.

Key words: experimental study, flow pattern, hydro-automatic flap gate, velocity of flow

INTRODUCTION

In water conservancy projects, sluice gates have been widely used for retaining water (Vijay *et al.* 2016). As a type of water-retaining construction, there is more than one hundred years of history for the existence of the bottom shaft driving flap gate, a form of dam gate with special structures. Also the bottom shaft driving flap gate is a kind of plane steel gate. The bottom shaft driving flap gate does not have a bottom gate slot and a side door slot; rather, it has a structure of a door leaf rotating around an axis. The bottom shaft driving flap gate is composed of the door leaf, bottom horizontal axis fixed at the bottom end of the door leaf, the bottom bearing, MGA (Metal Gear Alloy) self-lubricating bearings, a bottom water closing seal, a side water closing seal, a crank arm axis, a waterproof case device between the bottom axis and gate chamber, an integrated hydraulic driving device, hydraulic locking devices, etc. A hydraulic hoist is the driving device, and the two driving devices are arranged in the driving room on both sides of the dam, rotating through the bottom rotation axis driven by the crank arm to support the bottom rotation axis to rotate on the shaft seat, which drives the bottom shaft driving flap gate leaf fixed on the bottom rotating shaft. As the gate leaf can perform dam opening, dam closing, and other actions timely, smoothly, and reliably, according to the requirements, it can effectively guarantee river water storage, flood discharge, overflow, sailing, etc. The bottom shaft driving flap gate is shown in Figure 1.

Water Practice & Technology Vol 15 No 2
doi: 10.2166/wpt.2020.016

Figure 1 | Bottom shaft driving flap gate schematic diagram.

Compared with the traditional gates, the main performance advantages of the bottom shaft driving flap gate are shown in the following:

- Either to close the dam for water storage, or open the dam for flood drainage, one can let the water flow through the top of the dam to form the landscape effect of an artificial waterfall.
- MGA self-lubricating composite material is used for the bearing, this material can run in water for several years without any addition of lubricating oil, and will not rust.
- Based on the use of a hydraulic drive with a lock function, the dam can be locked at any angle to achieve the functions of dam decreasing or dam lifting, water level adjustment, and other functions. There will be no occurrence of displacement.
- With the use of advanced automation and network technology, one can control the dam through the internet from anywhere in the world.
- It is easy to operate the dam by the bottom shaft driving flap gate, and there is no need for ancillary facilities, such as an oil pipeline, pumping stations, and others. The hoist room combines with the bridge piers which, basically, have no impact on the river and bridge landscape.
- The upstream water closing seal of the bottom shaft driving flap gate is at the round shaft. When the dam is erected or falls, the water closing seal does not separate from the surface of the round shaft, always retaining the sealed state for water closing. The side water closing seal works on the same principle; the water closing surface never leaves the side parapet, so sand accretion (mud) does not affect the lifting or decreasing of the steel dam.

To sum up, the advantages of the hydro-automatic flap gate (HFG) are easy operation, simple structure, attractive appearance, cheaper investment, simple installation and maintenance compared to traditional gates. HFG can form the landscape effect of a waterfall, and its structure is simple and reliable, it can also eliminate the aging, abrasion, rolling and tearing of water closing seal, and avoid gate rustiness.

Compared with conventional gates such as plane steel gates and radial gates, flap gates have a shorter construction period and lower cost for embedded metal parts, gate opening and closing equipment and concrete works. The investment cost of a flap gate is about 90% of that for conventional gates. The operation of the flap gate hydraulic system is flexible and can be controlled by a buoy switch for automatic operation. As such, it can also reduce labour costs and material resources in operation, thus reducing comparable operating costs by 40%–50%. Compared with conventional gates, flap gates have a larger discharge capacity and can smoothly discharge the water flow, upstream sediment, pebbles and floating objects to avoid water blockage. It can effectively reduce maintenance costs caused by sediment blockage (maintenance cost reduction by 15%–25%). As long as the dam sector structure and hydraulic system are normally maintained, the flag gate's durability is longer than that of conventional gates.

Water Practice & Technology Vol 15 No 2
doi: 10.2166/wpt.2020.016

The flap gate is a low head water retaining structure and is widely used in water conservancy irrigation, hydroelectric power generation, urban landscaping and other aspects.

In the process of the design, construction, and operation management of river and water control projects, there will be many complex problems related with water. It not only has important academic significance, but also relates to key technologies of the project, so river problem research has important meaning. Vijay *et al.* (Vijay *et al.* 2016) conducted the design and evaluation of an integrated fiber reinforced polymer (FRP) composite wicket gate, and the authors introduced the advanced method of FRP to study the issues of hydraulic gates. It is also well-known that FRP is a cost-effective method to achieve the physical and performance requirements in engineering (Soti 2014; Rossum 2015). Experimental studies were conducted on a prototype for the Assiut Barrage by Mohamed F. Sauida (Kazemzadeh-Parsi 2014), to simulate flow scenarios to study experimentally and verify empirically the different parameters affecting the discharge through submerged multiple sluice gates. A prediction model for computing the coefficient of discharge of the sluice gates is developed using multiple regression analysis. Bijankhan (Belaud *et al.* 2014; Bijankhan *et al.* 2017) used submerged experimental velocity profiles to study the sluice gate, and his results showed that classical energy-momentum methods (EM) cannot accurately compute the flow rate due to high submergences, but when applying the interaction of the energy correction factors and head loss values, a more accurate head-discharge can be achieved. Hu *et al.* (Hu *et al.* 2011) have done research into a columnar reversing gate based on hydraulic calculation principles, and they built an FEM model of the columnar reversing gate to calculate its natural vibration properties. Kholopov *et al.* (Kholopov *et al.* 2016) conducted an optimal design of hydraulic gates in their paper, and the out-form volume was implemented in Kholopov's research so that the optimal form could be calculated for a girder of uniform cross-section. The hydraulic girder calculations have been widely used in many authors' studies (Gu & Yan 2011; Cui & Jiang 2014; Mavromatidis 2015).

As a new hydraulic gate, so far the bottom shaft driving flap gate has not yet seen mature engineering application examples like the hydraulic self-control flap gate. This type of gate will change the upstream plane and the downstream flow field during the opening and closing processes, thereby affecting the upstream and downstream gate water level. Meanwhile, the turbulent flow next to the gate is very complicated under different operating conditions, and there will be a great difference in water flow form. Therefore, in order to ensure the normal use of the gate and safety of hydraulic engineering, the engineering and technical personnel have to predict the motion laws of upstream and downstream water flows and sediment. In previous studies, the model test is a common method for converting test results to physical objects, so the study of the bottom shaft driving flap gate water flow pattern in this paper can not only verify the rationality of this type of gate flow pattern, but can also offer a reference for the application study of similar projects.

MATERIALS AND METHODS

There is a new type of hydro-automatic flap gate in the real world pending for construction, which will be located in the Ancient Yellow River. Therefore, this project is taken as the case study in this paper in order to analyze the distribution of flow velocity and hydraulic design rationality of the new bottom shaft driving flap gate. Also, the flow velocity measurement and forecast under different discharges and water levels near the gate were required to determine the best operation mode for the gate. The overall length of this water control project is about 313.5 m. The upstream river width is 110 m, with a length of 170 m.The downstream river width is 100 m, with a length of 80 m. The upstream connected segment is 19.84 m, and the downstream connected segment is 32.86 m. The length of the gate chamber segment is 10.8 m, with a net width of 18 m. There is an overflow dam located on each side of the gate chamber, with a horizontal range of 20 m, respectively.

Water Practice & Technology Vol 15 No 2
doi: 10.2166/wpt.2020.016

Experimental setup

In a physical model experiment, the water flow must be similar to the actual flow, thus the gravity similarity criterion is adopted to ensure that all kinds of hydraulic phenomena are similar. Gravity similarity criterion according to the Froude criterion is shown below.

$$F_r = v_r/\sqrt{g_r l_r} = 1 \tag{1}$$

Based on the actual project size and layout, a maximum model scale is selected in the Testing Hall to enhance the reliability of the physical model experiment. Model geometric scale was 1:20, and other hydraulic characteristics are shown in the following:

Geometric scale: $\lambda_r = \dfrac{l_p}{l_m} = 20$

Velocity ratio: $\mathrm{V_r} = \lambda_\mathrm{r}^{1/2} = 4.472$

Time scale: $T_r = \lambda_r^{1/2} = 4.472$

Discharge scale: $Q_r = \lambda_r^{5/2} = 1788.854$

Roughness scale: $n_r = \lambda_r^{1/6} = 1.648$

l: length.
r: rate of the practical value to model value.
p: practical value.
m: model value.

According to the geometric scale of 1:20, the overall model length is about 15.675 m. The upstream river width is 5.5 m, with a length of 8.5 m. The downstream river width is 5.0 m, with a length of 4.0 m. The upstream connected segment is 1.0 m, and the downstream connected segment is 1.643 m. The length of the gate chamber segment is 0.54 m, with a net width of 0.9 m. Roughness of the prototype is $n_p = 0.011 \sim 0.020$, and it is made of reinforced concrete. As such, the roughness of the physical model is $n_m = \frac{0.011 \sim 0.020}{1.648} = 0.0067 \sim 0.0121$. In accordance with this range, the calcareous plates ($n_m = 0.007 \sim 0.010$) are used to make the physical model, the gate is made of stainless steel. The hydraulic model is shown in Figure 2.

Table 1 is the inlet conditions for the prototype, and Table 2 is the inlet conditions of velocity and water depth for the physical model experiment.

Flow velocity distribution and flow direction of the sections with different water levels under various conditions are recorded by measuring points in the experiment. Corresponding water flow

Figure 2 | Overall layout of the physical model.

Water Practice & Technology Vol 15 No 2
doi: 10.2166/wpt.2020.016

Table 1 | Inlet conditions analysis table (according to prototype size)

	Conditions	Discharge (m^3/s)	Water depth of upstream gate (m)	Water depth of downstream gate (m)
Condition 1	Once in 20 years	87	3.00	2.87
Condition 2	Once in 50 years	101	3.088	2.928
Condition 3	Once in 100 years	111	3.2	3.01

Table 2 | Inlet conditions for physical model experiment

	Conditions	Discharge (m^3/s)	Water depth of upstream gate (m)	Water depth of downstream gate (m)
Condition 1	Once in 20 years	0.0486	0.15	0.1435
Condition 2	Once in 50 years	0.0565	0.1544	0.1464
Condition 3	Once in 100 years	0.062	0.16	0.1505

characteristics are observed in the surface layer and middle layers. The experiment sets up 13 sections, and each section is arranged with up to 45 measuring points (each section contains 5 layers, each layer contains about 9 measuring points), as shown in Figure 3. The specific measurement stratification is shown in Table 3.

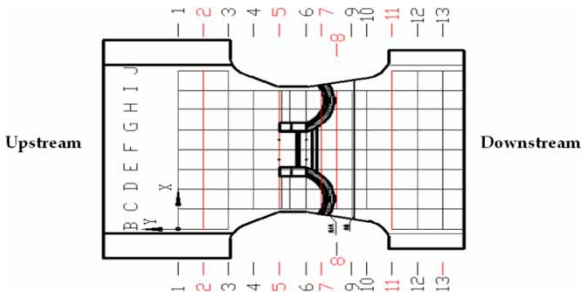

Figure 3 | Test sectional distribution chart (X-Y coordinate system is added in the figure).

Table 3 | Hierarchical arrangement table of measuring points

Conditions	Distance from measuring point to base plate (m)				
Condition 1	0.7 (0.035)	1.4 (0.07)	2.1 (0.105)	2.8 (0.14)	3.0 (0.15)
Condition 2	0.618 (0.031)	1.236 (0.062)	1.854 (0.093)	2.47 (0.1235)	3.088 (0.1544)
Condition 3	0.64 (0.032)	1.28 (0.064)	1.92 (0.096)	2.56 (0.128)	3.2 (0.16)

Note: Distances in physical model experiment are in parentheses.

Measurements and experimental device for hydraulic model

Measurements

Discharge measurement. The discharge of the model is measured by an intelligent electromagnetic flow meter, and the flow rate is controlled by a gate valve, a pipeline pump and a three-phase asynchronous motor.

Flow velocity measurement. For measuring the velocity distribution under different working conditions, 13 test sections are set in the physical model within the scope of the upstream and

Water Practice & Technology Vol 15 No 2
doi: 10.2166/wpt.2020.016

downstream. Each section is provided with spiral sensors to measure the velocities of 4–5 water-layers. In the upstream connected segment and downstream connected segment, the test sections' spacing was 0.5 m. In the gate chamber section, the test sections' spacing was 0.3 m. A multifunctional tachometer is used in the experiment, and test precision is $\pm 2\%$.

Flow pattern measurement. Specified plastic particles are used to observe surface flow pattern, and the bottom flow pattern is showed by chemical tracer method. This measurement can clearly reveal the water's reflux and swirl.

Measurement of water depth. Water level difference and water depth are obtained by level gauge and steel ruler with a connected pipe.

Experimental device

Discharge measuring equipment. The discharges are measured combining different flows with water levels, and the flow rate is controlled by the gate valve. The discharge is measured by electromagnetic flow meter.

Flow rate measuring equipment. Flow rate measuring equipment is a multifunctional tachometer with spiral sensors, which is manufactured in Nanjing Research Institute of Water Conservancy. The data acquisition interval is 10 seconds, and the test precision is $\pm 2\%$.

Circulating water supply system

The physical model is composed of water tanks, upstream section, gate chamber segment, downstream section, underground pool and circulating water supply system. A water tank with a constant water head is set in the physical model's upstream, and such a water tank is also set in the downstream. Then pumps and UPVC pipes are used to carry the water from the underground pool into the water tank, forming a circulating water supply system.

RESULTS AND DISCUSSION

Physical model experiment measurement results

The velocity vector is marked on the below charts. Figures 4–6 are the flow velocity distribution charts under the flood conditions occurring once in 20 years, once in 50 years and once in 100 years.

The flow regimes of the bottom and surface of the physical model under conditions of once in 20 years, once in 50 years, and once in 100 years are shown in Figures 4–6. Water flow from the upstream after entering through the gate upstream segment is relatively stable, and when the flow approaches the hoist chamber, the flow cross-section size changes, causing the water flow to gradually move toward the central axis. A small part of the water flow moves to both sides of the dam and forms a whirlpool with micro rotational speed. Two tiny swirling flows are formed at each side of the opening and closing chamber. After going through the chamber section, most of the water streams flow towards the downstream, and there is a small part of the water streams affected by the increase of the overflow section, forming raceways on either side of the river.

Water Practice & Technology Vol 15 No 2
doi: 10.2166/wpt.2020.016

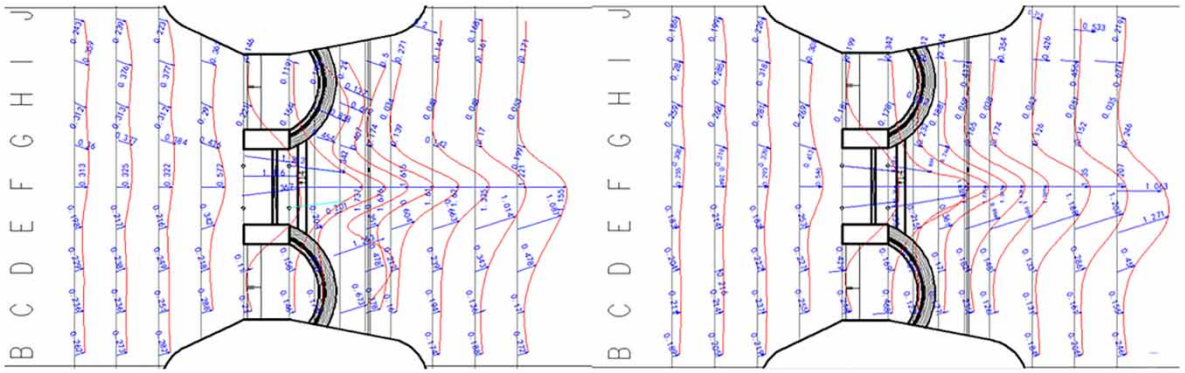

Figure 4 | Flow velocity distribution chart of bottom and topmost layer under the flood condition of once in 20 years.

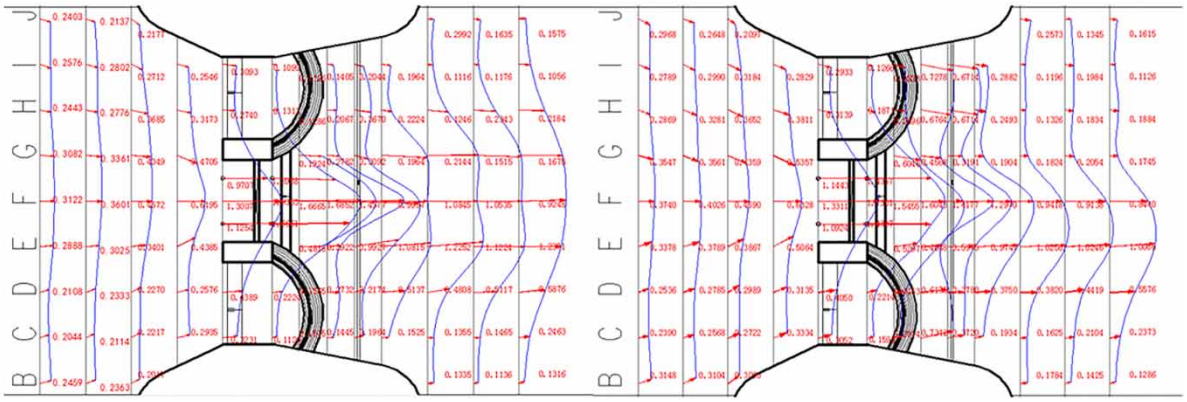

Figure 5 | Flow velocity distribution chart of bottom and topmost layer under the flood condition of once in 50 years.

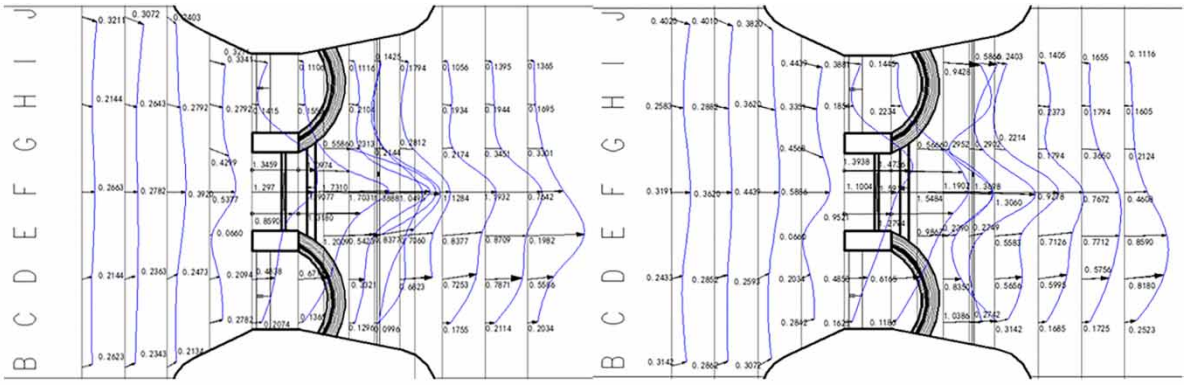

Figure 6 | Flow velocity distribution chart of bottom and topmost layer under the flood condition of once in 100 years.

Analysis of flow velocity measurement results

We select the flood condition of once in 50 years as an example to discuss the space-time change laws of flow velocities of the representative test sections of upstream section (2–2), sections near pier (5–5, 7–7, 8–8), and downstream section (11–11). These sections are marked in red in Figure 3, and they are our research focus.

Based on Figure 5, the velocity of the middle position of the physical model is relatively large, and the range of the flow velocity of the model is small, and the velocity direction gradually shifts to the

Water Practice & Technology Vol 15 No 2
doi: 10.2166/wpt.2020.016

central axis. The reason why the flow velocity had no obvious change is due to the unchanged cross-section in the upstream part. Because of the viscous effect of the bottom plate and side walls, the velocities near both sides of the model are slightly smaller than that of the middle position. Then the water flow gradually shifts to the central axis owing to the influence of cross section contraction near the gate. At the same time, it can be seen that the velocity decreases gradually with increasing depth because the flow velocity is affected by the sidewall effect of the model bottom plate.

It can be seen that the velocity distributions of sections near the pier are not uniform, and the velocity of the middle section is obviously greater than the velocities near both sides. The cause of this phenomenon is mainly the reduction in cross-section at the pier, resulting in the flow velocity increasing rapidly as the flow flux is a constant. The centerline velocity of the top measuring point (3.088 m) of section 5–5 is not the biggest, and it is less than the velocities of the measuring points of other layers. The reason is that the top layer of 5–5 is above the pier's top, so the water flow is affected by the blocking action of the pier, resulting in a smaller velocity. Through the analysis, the reason for the flow velocity changes of the topmost measuring points is that the sectional water level is much higher than the overflow dam, forming a larger water level drop to form a large flow velocity. The 8–8 sectional flow velocity distribution change is more dramatic compared to the 7–7 sectional flow velocity. This is mainly because the 8–8 cross-section is downstream of the overflow dam. After that, the upper part of the water level forms a drop. There is a relatively large water flow passing through the 8–8 cross-section, and there is a steep slope at the front end of the base plate which, to a certain degree, increases the flow velocity of the cross-section. As such, there is a dramatic change in the flow velocity under the combined effect of the large water flow and steep slope. However, the above two cross-sections are still of the situation that the central flow velocity is much greater than the flow velocity on both sides. The bottom flow velocities of 7–7 section and 8–8 section are all greater than that of the top layer flow, mainly because of the existence of a steep slope at the bottom of the downstream side of the gate, increasing the flow velocity at the bottom.

Section 11–11 is in the downstream section of the gate, and the velocity of the middle position is relatively large. In the center of the model, the velocity of the top is still bigger than the velocity of the bottom, showing that the steep effect still influences the flow speed. At a distance of 10 m and 70 m at the X axis, the flow rate is minimal, possibly due to the vortex generated.

The main difference occurs at the gate pier contraction segment and downstream segment; that is to say, the blocking effect of the gate pier seems to be bigger than expected, and the gate pier's effect on water flow will be studied in the future. Then there is a hydraulic drop at the downstream gate because we have set up a steep slope between the downstream segment and stilling basin. Hydraulic drop is a type of local phenomena found in open channel flow. It is a rapid change in the depth of flow from a high stage to a low stage that results in a steep depression in the water surface. The steep slope and stilling basin are mainly used to alleviate the high water momentum of hydraulic drop. As such, the steep slope could decrease the water flow rate, and this is another reason why the flow velocity obtained from the experiment is smaller.

The common feature of each working condition is that the upper flow state is more complicated than the bottom flow state, and the flow velocity changes more severely according to Table 4. Then the velocity of the water flow of once in 20 years is the smallest. For the once in 50 years, the topmost layer of water flow is obviously more torrent than the bottom water flow, resulting in a larger vortex. The water flow of once in 100 years is the most urgent and its vortex is greatest.

CONCLUSIONS

The bottom shaft driving flap gate boasts the advantages of landscape benefit, self-lubricating composite material, water level adjustment, networked control, and easy operation without sand accretion.

Water Practice & Technology Vol 15 No 2
doi: 10.2166/wpt.2020.016

Table 4 | Flow velocity distribution of bottom and topmost layers under three flood conditions

	Flow velocities of once in 20 years (m/s)		Flow velocities of once in 50 years (m/s)		Flow velocities of once in 100 years (m/s)	
Test sections	Bottom layer	Topmost layer	Bottom layer	Topmost layer	Bottom layer	Topmost layer
1	0.231	0.279	0.257	0.304	0.256	0.307
2	0.245	0.288	0.272	0.319	0.264	0.325
3	0.258	0.291	0.304	0.341	0.274	0.351
4	0.324	0.358	0.379	0.434	0.303	0.34
5	0.479	0.67	0.677	0.698	0.667	0.667
6	0.512	0.563	0.8	0.828	0.771	0.801
7	0.535	0.541	0.413	0.518	0.821	0.731
8	0.511	0.521	0.431	0.73	0.733	0.751
9	0.482	0.518	0.532	0.614	0.621	0.611
10	0.47	0.434	0.48	0.536	0.58	0.561
11	0.422	0.349	0.423	0.458	0.483	0.424
12	0.473	0.383	0.402	0.3838	0.535	0.428
13	0.485	0.448	0.419	0.379	0.337	0.411

However, as a new hydraulic gate, so far the bottom shaft driving flap gate has not received due attention and there are almost no engineering application examples. Therefore, through physical model experiment, this paper completed the measurement and analysis of the flow velocity and flow pattern on the bottom shaft driving flap gate project under three flood conditions to study the turbulent flow next to the gate. On the basis of flow velocity distribution charts, it was concluded that the water flow situation under the flood condition of once every 20 years is relatively gentle, the water flow situation of flood condition occurring once every 50 years is very similar to that of the flood condition occurring once every 100 years, and the whirlpools of these three flood conditions mainly occur in the downstream central location. This is because the water flows through the overflow dam (once every 50 years and once every 100 years) will form a water level difference, causing the downstream water level to be relatively disordered. According to the flow velocity cloud pictures of the three flood conditions, the largest flow velocity mainly occurs in the vicinity of the narrowing segment of the pier section.

ACKNOWLEDGEMENTS

This work was supported by the Project funded by China Postdoctoral Science Foundation (Grant No. 2019M663121).

REFERENCES

Belaud, G., Cassan, L. & Baume, J. P. 2014 Discussion of 'Revisiting the energy-momentum method for rating vertical sluice gates under submerged flow conditions' by Oscar Castro-Orgaz, Luciano Mateos, and Subhasish Dey. *Journal of Irrigation and Drainage Engineering* **140**(7), 07014019.

Bijankhan, M., Kouchakzadeh, S. & Belaud, G. 2017 Application of the submerged experimental velocity profiles for the sluice gate's stage-discharge relationship. *Flow Measurement and Instrumentation*. doi:10.1016/j.flowmeasinst.2016.11.009.

Cui, C. Y. & Jiang, B. S. 2014 A morphogenesis method for shape optimization of framed structures subject to spatial constraints. *Engineering Structures* **77**, 109–118. doi:10.1016/j.engstruct.2014.07.032.

Gu, H. & Yan, G. H. 2011 Analysis of vibration mode of hydraulic gate structure. *Advanced Materials Research* **199–200**, 966–972.

Water Practice & Technology Vol 15 No 2
doi: 10.2166/wpt.2020.016

Hu, Y., Wang, M., Wang, M. M., Ge, S., Niu, W. & Xu, T. 2011 Hydraulic calculation and dynamic analysis of columnar reversing gate. *Water Science and Engineering* **4**(3), 294–304.

Kazemzadeh-Parsi, M. J. 2014 Numerical flow simulation in gated hydraulic structures using smoothed fixed grid finite element method. *Applied Mathematics and Computation* **246**, 447–459.

Kholopov, I. S., Balzannikov, M. I., Alpatov, V. Y. & Soloviev, A. V. 2016 Girders of hydraulic gates optimal design. *Procedia Engineering* **153**, 277–282.

Mavromatidis, L. E. 2015 A review on hybrid optimization algorithms to coalesce computational morphogenesis with interactive energy consumption forecasting. *Energy and Buildings* **106**, 192–202. doi:10.1016/j.enbuild.2015.07.003.

Rossum, S. V. 2015 *Road Toward A Standardized Lock Gate*. MS Thesis, TU Delft, Delft University of Technology.

Soti, P. R. 2014 *Advanced Composites for Design and Rehabilitation of Hydraulic Structures*. MS Thesis, West Virginia University.

Vijay, P. V., Soti, P. R., GangaRao, H. V. S., Lampo, R. G. & Clarkson, J. D. 2016 Design and evaluation of an integrated FRP composite wicket gate. *Composite Structures* **145**, 149–161.